Special Issue: Advances in Cardiometabolic and Coronary Artery Disease

Journal of INTERNATIONAL MEDICAL RESEARCH

Journal of International Medical Research
48(1) 1–12

DOI: 10.1177/0300060519839625
journals.sagepub.com/home/imr
SAGE

Computer-assisted prediction of atherosclerotic intimal thickness based on weight of adrenal gland, interleukin-6 concentration, and neural networks

Ling-bing Meng[1,*], Yang-fan Zou[2,*], Meng-jie Shan[3], Meng Zhang[4], Ruo-mei Qi[5], Ze-mou Yu[6], Peng Guo[7], Qian-wei Zheng[1] and Tao Gong[1]

Abstract

Objective: Atherosclerosis (AS) is the main pathological basis of ischemic cardio-cerebrovascular diseases, and the intimal thickness (IT) of large arteries is regarded as a powerful evaluation indicator for AS. We established an effective neural network model for automatic prediction of the IT and analyzed the high-risk warning indicators of IT.

Methods: The weight of the left adrenal (WLA) was evaluated. The serum interleukin-6 (IL-6) concentration was measured by enzyme-linked immunosorbent assay. The statistical methods included neural network modeling, a cubic spline interpolation algorithm, Spearman's rho test, and linear fit.

Results: Thirty-seven rabbits were classified into a control group (n = 11), high-fat diet group (n = 13), and high-fat diet plus chronic stress group (n = 13). The neural network model was

[1]Neurology Department, Beijing Hospital, National Center of Gerontology, Beijing, P.R. China
[2]Department of Neurosurgery, Chinese PLA General Hospital-Sixth Medical Center, Beijing, P.R. China
[3]MOH Key Laboratory of Systems Biology of Pathogens, Institute of Pathogen Biology, Chinese Academy of Medical Sciences and Peking Union Medical College, Beijing, P.R. China
[4]School of Energy Power and Mechanical Engineering, North China Electric Power University, Baoding, Hebei, P. R. China
[5]MOH Key Laboratory of Geriatrics, Beijing Hospital, National Center of Gerontology, Beijing, P.R. China
[6]Department of Neurology, Peking University First Hospital, Beijing, P. R. China
[7]Department of Orthopedics, The Fourth Hospital of Hebei Medical University, Shijiazhuang, Hebei, P.R. China

*These authors contributed equally to this work.

Corresponding author:
Tao Gong, Neurology Department, Beijing Hospital, National Center of Gerontology, No. 1 Dahua Road, Dong Dan, Beijing 100730, P.R. China.
Email: mac0852@163.com

successfully established and verified by comparing the predicted IT with the actual IT. The high-risk warning indicator of IT was identified as follows: $0.445\,g < WLA < 0.610\,g$ and $60\,ng/L < IL\text{-}6 < 80\,ng/L$.

Conclusions: The neural network model based on WLA and IL-6 could predict the IT of AS. When $0.445\,g < WLA < 0.610\,g$ and $60\,ng/L < IL\text{-}6 < 80\,ng/L$, the risk to developing AS is very high.

Keywords

Cardio-cerebrovascular diseases, atherosclerosis, intimal thickness, neural network model, interleukin-6, weight of adrenal

Date received: 20 October 2018; accepted: 25 February 2019

Introduction

As the aging of society has progressed, the prevalence of cardio-cerebrovascular diseases (CCVDs) has significantly increased.[1] CCVDs have become one of the most disabling and lethal diseases worldwide, with ischemic CCVDs accounting for the majority. Atherosclerosis (AS) is the main pathological basis of ischemic CCVDs, and the intimal thickness (IT) is a key evaluation indicator for AS.[2–4] The endarterium is normally very thin, and the endovascular cavity contains a layer of endothelial cells and a layer of red continuous elastic membrane. A critical reason for the inability to effectively control ischemic CCVDs is that the current medical technology cannot successfully prevent the physiological and pathological changes that affect the IT.[5,6] Biological, environmental, genetic, physical, and other factors can collectively promote IT-related lesions. Increasingly more studies are showing that chronic stress (CS) plays a key role in changes of the IT.[7–9]

CS refers to the nonspecific systemic reactions that occur when the body is stimulated by various internal and external negative factors for a long period of time. Long-term CS events are crucial predisposing factors for physical and mental diseases. Approximately 40% of cases of AS in patients without traditional risk factors are associated with CS.[10,11] Epidemiological investigations and laboratory studies have shown that high-intensity stress has become a significant factor in the pathogenesis of AS.[12] However, the mechanism underlying the occurrence and development of CS-induced AS remains unclear. Heidt et al.[13] showed that CS promotes the formation of AS by overactivation of the hypothalamic-pituitary-adrenal (HPA) axis and is closely related to inflammatory factors such as interleukin-6 (IL-6).

The HPA axis is an important part of the neuroendocrine system. It is a neuroendocrine regulatory axis with both direct and feedback effects. The HPA axis is also involved in controlling the response and activity of the CS system and regulating numerous physical activities such as emotional responses, the immune system, and energy storage and consumption.[14] When the body perceives an imbalance in its internal environment after exposure to long-term CS, the HPA axis is involved in controlling the body's stress response and regulating the metabolism of various energy sources and substances in the body. Okutsu et al.[15] showed that a variety of psychological and physiological stresses can lead to hyperfunction of the HPA axis and that hyperactivity of the HPA axis is the key point of bodily damage caused by stress. The adrenal gland, as the target organ of the HPA axis, is stimulated by adrenocorticotropic hormone secreted by the pituitary gland during long-term CS. Corresponding physiological and pathological changes then occur, followed by changes in the volume and morphology of the adrenal gland.[16]

The secretion of IL-6 can increase as a result of long-term CS.[17] IL-6 is a cytokine that stimulates the growth and differentiation of B-lymphocytes, and it serves as a growth factor for hybridomas and plasmacytomas. As an important inflammatory mediator in the body, IL-6 can stimulate immune cell proliferation and differentiation and enhance immune cell function. IL-6 is mainly produced in vascular endothelial cells, monocyte macrophages, fibroblasts, T lymphocytes, B lymphocytes, and keratinocytes.[18] Under CS, the secretion of IL-6 is increased. This results in the release of monocyte chemotactic protein, promotion of monocyte migration into the vascular endothelium, and destruction of the normal vascular endothelial structure and function. All of these changes intensify the inflammatory reaction and promote the occurrence of AS.[19]

Most of the currently available prediction models of CCVDs were established based on qualitative lifestyle risk factors with the aim of assessing risk probability in the population.[20–22] However, few studies have used quantitative risk factors to establish a prediction model and determine the high-risk warning range for changes in the IT under long-term CS. Therefore, the present study was performed to establish a predictive model of IT changes in patients with AS and analyze the high-risk warning range of changes in the IT. This was accomplished by establishing a CS animal model, using a neural network and cubic spline interpolation algorithm, and utilizing the adrenal gland weight and blood IL-6 concentration. The results of this study will provide a scientific basis for the development of guidelines for the prevention and treatment of CCVDs.

Materials and methods

Animals and diet

Thirty-seven New Zealand white rabbits (approximate age, 3 months; mean body weight, 3.0 ± 0.2 kg) were obtained from the Institute of Laboratory Animal Sciences of the Chinese Academy of Medical Sciences and Peking Union Medical College. During the first week of the study, the rabbits were allowed to adapt to the new environment (25°C $\pm$ 2°C; relative humidity, 60% $\pm$ 2%). All rabbits were raised alone in cages with free access to food and water.

The rabbits were randomly divided into three different groups: the control group ($n = 11$), the high-fat (HF) diet group (HF group, $n = 13$), and the HF diet plus CS group (HF+CS group, $n = 13$). Ethical approval of this study was provided by the Animal Care and Use Committee. All procedures were in accordance with the ethical standards of the institutional ethical committee and with the 1964 Helsinki declaration and its later amendments. All applicable international, national, and/or institutional guidelines for the care and use of animals were followed.

CS assay

CS was induced as described in a previous report.[23] First, noise stimulation was performed by sounding an alarm at about 110 decibels (dB) for 5 seconds, followed by 5 minutes of silence; this was repeated for 3 hours. Second, flash and alarm stimulation was performed by implementing a flash plus the continuous alarm (about 85 dB) for 2 hours after the lights were turned off in the laboratory. Third, constraint stimulation was performed by limiting the rabbit's activity with a rabbit box for 3 hours. Fourth, lighting stimulation was performed by implementation of continuous lighting after 19:00. Fifth, fear stimulation was performed by hanging the cages, and the cages inclined when the rabbits moved slightly. This step was continued for 2 hours. Finally, water was withheld for 24 hours, and food was withheld for the next 24 hours. The CS period was 7 days, and one cycle was implemented per month. The procedure was continued for 2 months.

Weights of right and left adrenal glands

The bilateral adrenal glands were separated from all rabbits. Excess connective tissue was removed with an ophthalmic tweezers, and the clean bilateral adrenal glands were weighed with an electronic scale. The weight of the right adrenal (WRA) and weight of the left adrenal (WLA) were acquired.

Detection of serum IL-6 concentration

Blood samples were collected with the rabbits under chloral hydrate anesthesia. An ethylenediaminetetraacetic acid anticoagulant tube was used to store 0.4 mL of blood. IL-6 was detected by a commercially available enzyme-linked immunosorbent assay kit (R&D Systems, Minneapolis, MN, USA).

Measurement of IT of abdominal artery

After blood collection, the abdominal artery was dissected and cut into segments. Part of the artery was fixed in 4% polyformaldehyde solution and processed for paraffin embedding and sectioning. The abdominal artery was then cut into 6-μm-thick transverse sections and stained with hematoxylin and eosin. The IT of the atherosclerotic plaques was measured in hematoxylin- and eosin-stained sections of the abdominal artery under a microscope (Axio Zoom.V16; ZEISS, Oberkochen, Germany) using Image-Pro Plus 5.0 software (Media Cybernetics, Rockville, MD, USA). The IT was calculated as the radius bounded by the inner elastic membrane minus the radius of the lumen.

Statistical analysis

All statistical analyses were conducted using SPSS software, version 21.0 (IBM Corp., Armonk, NY, USA). Spearman's rho test was executed to compare the adrenal weight and serum IL-6 concentration for the correlation analysis. A cubic spline interpolation algorithm was implemented to analyze the high-risk warning range of the IT. A p-value of <0.05 was considered statistically significant.

Neural network modeling

A neural network is a computing system that utilizes a large number of connected artificial neurons to simulate the computing capacity of a biological system. A neural network is composed of many simple processing elements known as neurons. In a neural network, each neuron links connections to other neurons through direct communication. Each neuron has an associated weight, and the network is used to solve the problem of information, as shown in the model below.

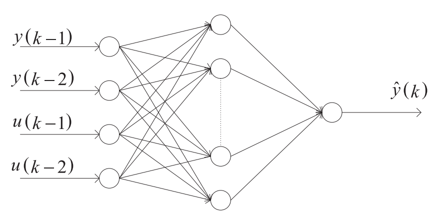

The basic algorithm of neural network modeling is as follows.

1. All weights are given at random $\{w_{ji}\}\{v_{ih}\}$, including the threshold value, which is generally in the random of $\{-1, 1\}$.
2. Based on the $s(k)$, calculate:

$$net_i^A(k) = \sum_{h=1}^{n+1} v_{ih} s_h(k), \quad i = 1 \ldots p \tag{3}$$

$$a_i(k) = \sigma\left(net_i^A(k)\right), \quad i = 1 \ldots p \tag{4}$$

Note: $s_{n+1}(k) = 1, \quad v_{in+1} = \theta_i$

3. Calculate:

$$y_j(k) = \sum_{j=1}^{p+1} w_{ji}(k) a_i(k), \quad j = 1 \ldots q \tag{5}$$

Note: $w_{jp+1} = r_j$

4. Calculate:

$$e_{yj}(k) = d_j(k) - y_j(k), \quad j = 1 \ldots q \tag{6}$$

$$e_{ai}(k) = a_i(k)\left(1 - a_i(k)\right) \sum_{j=1}^{q} w_{ji} e_{yj}(k), \quad j = 1 \ldots q \tag{7}$$

5. Train $\{w_{ji}\}\{v_{ih}\}$

$$\begin{aligned} w_{ji}(k+1) &= w_{ji}(k) - \eta a_i(k) e_{yj}(k), \\ & i = 1 \ldots p+1, \quad j = 1 \ldots q \\ v_{ih}(k+1) &= v_{ih}(k) - \eta e_{ai}(k) s_h(k), \\ & i = 1 \ldots p+1, \quad h = 1 \ldots n+1 \end{aligned} \tag{8}$$

6. Turn to (2), and train repeatedly.
7. Train stop.

The training group was randomly divided into training data and calibration data in a 7:3 proportion. There were 26 individuals in the training data and 11 individuals in the calibration data. Matlab8.3 was used to accomplish the normalization processing of variable values, network initialization, network training, and network simulation. The number of input neurons in the input layer was the same as the number of input variables; i.e., two. The hidden layer was designed as one layer, and the output layer was also designed for one layer. One output variable was the IT. The forecast model was then established with a hidden unit number of 6. When training to 5000 steps after repeated training, the falling gradient was 0, and the training speed was uniform. At the same time, the training error was 0.036839, and the R (relativity) value reached 0.94785.

Results

Strong association between WRA and WLA

Spearman's correlation coefficient analysis revealed that the IT was significantly associated with WRA ($p = 0.008$), WLA ($p = 0.002$), and IL-6 ($p = 0.023$) (Table 1). Spearman's correlation coefficient analysis and linear fit showed that WRA was positively associated with WLA ($R = 0.936$,

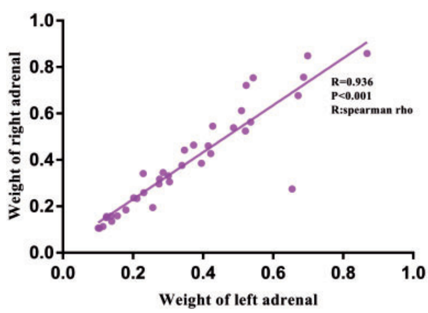

Figure 1. Linear correlation between the weight of the left adrenal and weight of the right adrenal.

$p < 0.001$) (Table 2, Figure 1). Therefore, for further analysis, the neural network model could consider one factor, such as WLA.

Table 1. Associations between intimal thickness and relevant metabolic characteristics.

	Spearman's rank correlation coefficient	
Characteristics	ρ^a	p-value
WRA	0.428	0.008*
WLA	0.487	0.002*
IL-6	−0.374	0.023*

[a]Spearman's rank correlation coefficient between intimal thickness and relevant characteristics.
ρ: Spearman's correlation coefficient. *Significant variables ($p < 0.05$).
WRA, weight of right adrenal; WLA, weight of left adrenal; IL-6, interleukin-6.

Neural network prediction model of IT

The neural network prediction model was successfully established, attaining the best training performance in which the mean squared error was 0.036839 at epoch 5000 (Figure 2(a)) and the R (relativity) was 0.94785 (Figure 2(b)).

The actual IT and predicted IT were compared to verify the veracity of the neural network prediction model. The variation trend of the predicted IT was similar to the actual IT (Figure 3(a)), and the R (relativity) was 0.872 ($p < 0.001$) based on Spearman's correlation coefficient analysis and linear fit (Figure 3(b), Table 3). Therefore, the neural network established in this study is worthy of mention.

Table 2. Associations between WRA and WLA.

Data	n	Mean	SD	R	p-value
WRA	37	0.35583	0.19908	0.936	<0.001*
WLA	37	0.38806	0.22099		

IT, intimal thickness; SD, standard deviation; R, Spearman's rank correlation coefficient; WRA, weight of right adrenal; WLA, weight of left adrenal. *Significant variables ($p < 0.05$).

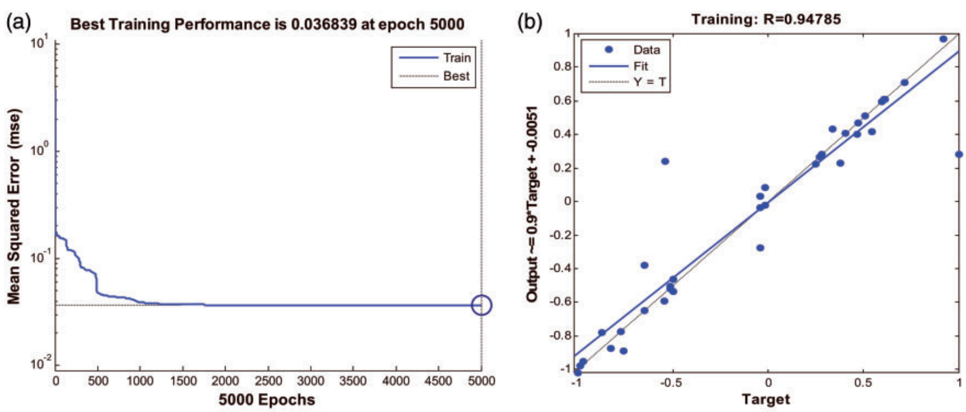

Figure 2. Neural network prediction model of intimal thickness in atherosclerosis. (a) The best training performance was 0.036839 at epoch 5000. (b) The final training model. The relativity was 0.94785.

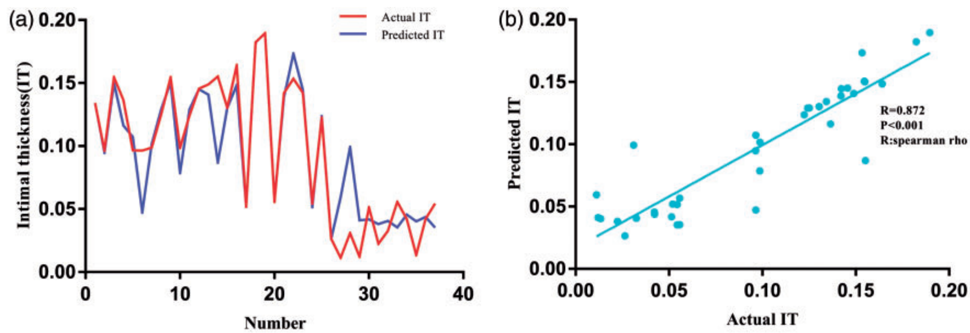

Figure 3. Verification of the neural network prediction model. (a) Variation trend of the predicted IT and actual IT. (b) Linear correlation between the predicted IT and actual IT. IT, intimal thickness.

Table 3. Comparison between the actual IT and predicted IT.

Data	n	Mean	SD	R	p-value
Actual IT	37	0.095944231	0.054	0.872	<0.001*
Predicted IT	37	0.095944289	0.049		

IT, intimal thickness; SD, standard deviation; R, Spearman's rank correlation coefficient.
*Significant variables ($p < 0.05$).

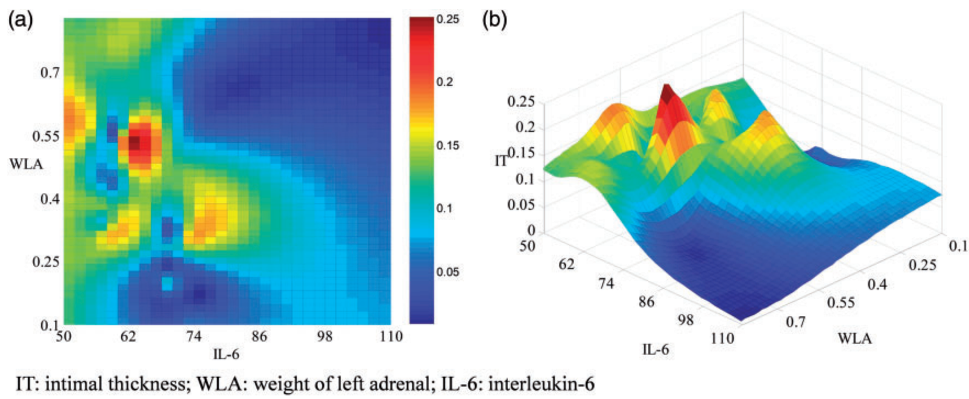

Figure 4. High-risk warning range of intimal thickness in atherosclerosis. The color represents the intimal thickness: red represents high, green represents medium, and blue represents low. (a) Planform. (b) Three-dimensional stereogram.

High-risk warning range of IT

Through the cubic spline interpolation algorithm, we identified the high-risk warning indicator of the AS IT as follows: $0.445 < \text{WLA} < 0.610$ g and 60 ng/L < serum IL-6 concentration < 80 ng/L, presented as the color "red" in the planform (Figure 4(a)). In addition, a three-dimensional stereogram was created to observe the high-risk warning range vividly and intuitively (Figure 4(b)).

Discussion

This study showed that during long-term CS, the WLA, WRA, and serum IL-6 concentration were significantly correlated with the IT of AS. In addition, the change in WLA showed a significant positive correlation with WRA. Therefore, the prediction model of IT was successfully established using the neural network algorithm, WLA, and serum IL-6. By the cubic spline interpolation algorithm, the following high-risk warning range was obtained: $0.445\,g < WLA < 0.610\,g$ and $60\,ng/L <$ serum IL-6 concentration $< 80\,ng/L$.

Several mature CCVDs prediction models have been established, and the most mature model is the result of research by D'Agostino et al.[24] The predicted results of their study have been used in many countries as an important basis for formulating and revising guidelines for the prevention and treatment of hypertension and dyslipidemia. However, these models also have the following defects: most of the models used are Cox proportional risk regression models with generally weak extrapolation ability, and most of the predictors are qualitative lifestyle risk factors, which are greatly influenced by subjective factors.[20–22]

The prediction model established in the present study may compensate for the deficiencies mentioned above. First, the neural network model is a modern multivariate, nonlinear model. (1) Multivariate: The neural network is a computing system that uses a large number of connected artificial neurons to simulate the computing capacity of a biological system. (2) Nonlinear: The wisdom of the brain is a nonlinear phenomenon. Artificial neurons are in one of two different states, either activation or inhibition, and this behavior shows a nonlinear relationship in mathematics. The pathogenesis of diseases is a complex process affected by multiple factors. Traditional statistical methods often require normality and independence of variables, and the prediction of diseases is very limited. The advantages of neural network models are suitable for the prediction of disease risks.[2,25,26] Second, the prediction model was constructed using two quantitative indicators, the WLA and serum IL-6 concentration, which can effectively avoid the interference of subjective factors and can be explained by nervous system, endocrine, and inflammatory mechanisms. Additionally, some studies have used neural networks and quantitative indicators to predict other disease indexes.[25,27,28]

The adrenal gland is the terminal organ of the HPA axis, and changes in its weight also reflect the functional changes in the HPA axis to some extent. The hippocampus, which regulates the stress response, is the high regulatory center of the HPA axis.[29] The normal hippocampus inhibits activation of the HPA axis, and the hippocampal glucocorticoid (GC) receptor is sensitive and vulnerable to the stress response. The HPA axis plays an important role in lipid and glucose metabolism in the body.[30] In the normal physiological condition, GC exhibits negative feedback regulation of the HPA axis,[31] but under the condition of stress, the following changes occur: 1) the hippocampus is impaired; 2) the function of the HPA axis is enhanced; 3) the hypothalamic secretion of corticotropin-releasing hormone is excessive; 4) excessive corticotropin-releasing hormone stimulates increased pituitary secretion of adrenocorticotropic hormone; 5) GC secretion then becomes excessive, which can cause dysregulation of the negative feedback mechanism of the HPA axis; and 6) continued hyperfunction of the HPA axis ultimately results.[32] The plasma levels of catecholamines and glucagon are elevated during stress, and GC can synergize with them to increase the activity of protein lipase and hepatic lipase and accelerate the decomposition of fat, thereby increasing the free fatty acid content; this improves the synthesis of triglycerides and very-low-density lipoprotein in the liver, promoting the occurrence of hyperlipidemia.[33] However, elevated GC during stress affects signal transduction of insulin signaling in the body, causing insulin resistance while raising blood sugar levels by promoting hepatic gluconeogenesis and stimulation of glucagon secretion, leading to decreased glucose tolerance and promoting the development of type 2 diabetes. This in turn exacerbates the damage to the vascular endothelial cells and causes lipids to be deposited under the endothelium.[34]

Studies have shown that IL-6 is mainly produced by activated mononuclear macrophages and is related to the inflammatory reaction.[35,36] IL-6 can also stimulate the production of C-reactive protein in macrophages and promote platelet aggregation. Moreover, IL-6 can cause the proliferation of vascular smooth muscle cells, the progression of arteriosclerosis, and the development of plaques from stability to instability, leading to the occurrence of acute ischemic CCVDs. Studies have also shown that atherosclerosis is the result of an imbalance in endothelial cell repair ability and inflammation regulation.[2,37,38] The inflammatory reaction is derived from a combination of inflammatory cells, transmitters, and cytokines. Oxidized low-density lipoprotein activates vascular endothelial cells, reduces the synthesis of nitric oxide, and increases the expression of inflammatory factors. The inflammatory effect is thus significantly amplified, with serum IL-6 being the most common and important inflammatory cytokine.[39,40]

The present study had some limitations. The application of a neural network algorithm in the field of medicine has just started.[41,42] Some problems remain unsolved, such as the hypothesis test of the weight coefficient, the confidence interval of the weight coefficient, the epidemiological significance of the weight coefficient, and the selection of input variables. In the present study, 37 samples were used to train the code. All data were obtained from experimental animals, which were strictly and precisely controlled by the researchers. This was a preliminary theoretical exploration that provides insight for follow-up research; it has not reached the application level. In future clinical work, we will focus on collecting more patient-related information to verify the theory. To further verify the scientific and extrapolated nature of the model, a prospective multicenter controlled study should be conducted among a wide range of community populations to verify and improve the prediction model.[43,44]

Conclusion

The herein-described neural network model based on WLA and IL-6 could predict the IT of AS. When $0.445\,g < WLA < 0.610\,g$ and $60\,ng/L < IL\text{-}6 < 80\,ng/L$, the risk of developing AS is very high. Therefore, the combined predictive effect of the WLA and serum IL-6 concentration could be used as a diagnostic biomarker for the IT of AS in clinical practice. The neural network algorithm is a promising method for the prediction of AS.

Abbreviations

CCVDs, cardio-cerebrovascular diseases; AS, atherosclerosis; IT, intima thickness; CS, chronic stress; HPA, hypothalamic-pituitary-adrenal; IL-6, interleukin; HF, high-fat; dB, decibels; WRA, weight of right adrenal; WLA, weight of left adrenal; GC, glucocorticoid

Declaration of conflicting interest

The authors declare that there is no conflict of interest.

Funding

This work was supported by the National Natural Science Foundation of China (Number: 31271097).

ORCID iD

Meng-jie Shan http://orcid.org/0000-0002-3451-1103
Tao Gong http://orcid.org/0000-0002-9135-8619

References

1. Izzo C, Carrizzo A, Alfano A, et al. The impact of aging on cardio and cerebrovascular diseases. *Int J Mol Sci* 2018; 19: pii: E481.
2. Yoshida M, Higashi K, Kobayashi E, et al. Correlation between images of silent brain infarction, carotid atherosclerosis and white matter hyperintensity, and plasma levels of acrolein, IL-6 and CRP. *Atherosclerosis* 2010; 211: 475–479.
3. Jeevarethinam A, Venuraju S, Weymouth M, et al. Carotid intimal thickness and plaque predict prevalence and severity of coronary atherosclerosis: a pilot study. *Angiology* 2015; 66: 65–69.
4. Eroglu S, Sade LE, Polat E, et al. Association between serum gamma-glutamyltransferase activity and carotid intima-media thickness. *Angiology* 2011; 62: 107–110.
5. Toledo-Corral CM, Myers SJ, Li Y, et al. Blunted nocturnal cortisol rise is associated with higher carotid artery intima-media thickness (CIMT) in overweight African American and Latino youth. *Psychoneuroendocrinology* 2013; 38: 1658–1667.
6. Loureiro C, Campino C, Martinez-Aguayo A, et al. Positive association between aldosterone-renin ratio and carotid intima-media thickness in hypertensive children. *Clin Endocrinol (Oxf)* 2013; 78: 352–357.
7. Johnstone SE and Baylin SB. Stress and the epigenetic landscape: a link to the pathobiology of human diseases. *Nat Rev Genet* 2010; 11: 806–812.
8. Yang G, Lei Y, Inoue A, et al. Exenatide mitigated diet-induced vascular aging and atherosclerotic plaque growth in ApoE-deficient mice under chronic stress. *Atherosclerosis* 2017; 264: 1–10.
9. Mallika V, Goswami B and Rajappa M. Atherosclerosis pathophysiology and the role of novel risk factors: a clinicobiochemical perspective. *Angiology* 2007; 58: 513–522.
10. Black PH and Garbutt LD. Stress, inflammation and cardiovascular disease. *J Psychosom Res* 2002; 52: 1–23.
11. Golbidi S, Frisbee JC and Laher I. Chronic stress impacts the cardiovascular system: animal models and clinical outcomes. *Am J Physiol Heart Circ Physiol* 2015; 308: H1476–H1498.
12. Devaki M, Nirupama R and Yajurvedi HN. Chronic stress-induced oxidative damage and hyperlipidemia are accompanied by atherosclerotic development in rats. *Stress* 2013; 16: 233–243.
13. Heidt T, Sager HB, Courties G, et al. Chronic variable stress activates hematopoietic stem cells. *Nat Med* 2014; 20: 754–758.
14. Marissal-Arvy N, Batandier C, Dallennes J, et al. Effect of a high-fat–high-fructose diet, stress and cinnamon on central expression of genes related to immune system, hypothalamic-pituitary-adrenocortical axis function and cerebral plasticity in rats. *Br J Nutr* 2014; 111: 1190–1201.
15. Okutsu M, Lira VA, Higashida K, et al. Corticosterone accelerates atherosclerosis in the apolipoprotein E-deficient mouse. *Atherosclerosis* 2014; 232: 414–419.
16. Kyrou I and Tsigos C. Stress mechanisms and metabolic complications. *Horm Metab Res* 2007; 39: 430–438.
17. Wang J, Hodes GE, Zhang H, et al. Epigenetic modulation of inflammation and synaptic plasticity promotes resilience against stress in mice. *Nat Commun.* 2018; 9: 477.
18. Aguiló S, Garcia E, Arza A, et al. Evaluation of chronic stress indicators in geriatric and oncologic caregivers: a cross-sectional study. *Stress* 2018; 21: 36–42.
19. Zhang Y, Fan K, Liu Y, et al. Cathepsin C aggravates neuroinflammation involved in disturbances of behaviour and

neurochemistry in acute and chronic stress-induced murine model of depression. *Neurochem Res* 2018; 43: 80–91.
20. Patel J, Al Rifai M, Scheuner MT, et al. Basic vs More complex definitions of family history in the prediction of coronary heart disease: the multi-ethnic study of atherosclerosis. *Mayo Clin Proc* 2018; 93: 1213–1223.
21. Osawa K, Trejo MEP, Nakanishi R, et al. Coronary artery calcium and carotid artery intima-media thickness for the prediction of stroke and benefit from statins. *Eur J Prev Cardiol* 2018; 25: 1980–1987.
22. Wang H, Sun Y, Wang S, et al. Comparisons of the Framingham and ASCVD risk scores for coronary heart disease risk prediction in Chinese men. *Int J Cardiol* 2018; 266: 269.
23. Meng LB, Qi R, Xu L, et al. The more critical murderer of atherosclerosis than lipid metabolism: chronic stress. *Lipids Health Dis* 2018; 17: 143.
24. D'Agostino RB Sr, Vasan RS, Pencina MJ, et al. General cardiovascular risk profile for use in primary care: the Framingham Heart Study. *Circulation* 2008; 117: 743–753.
25. Atkov OY, Gorokhova SG, Sboev AG, et al. Coronary heart disease diagnosis by artificial neural networks including genetic polymorphisms and clinical parameters. *J Cardiol* 2012; 59: 190–194.
26. Ozbay Y, Kara S, Latifoglu F, et al. Complex-valued wavelet artificial neural network for Doppler signals classifying. *Artif Intell Med* 2007; 40: 143–156.
27. Stachowska E, Gutowska I, Dolegowska B, et al. Exchange of unsaturated fatty acids between adipose tissue and atherosclerotic plaque studied with artificial neural networks. *Prostaglandins Leukot Essent Fatty Acids* 2004; 70: 59–66.
28. Liu Y, Buendia-Rodriguez G, Penuelas-Rivas CG, et al. Experimental and computational studies of fatty acid distribution networks. *Mol Biosyst* 2015; 11: 2964–2977.
29. Zahorodna A, Tokarski K and Bijak M. [Electrophysiologic tests for testing the effects of antidepressant drugs and corticosterone on reactivity of serotonin receptors in the hippocampus]. *Postepy Hig Med Dosw* 2000; 54: 391–401.
30. Pan A, Keum N, Okereke OI, et al. Bidirectional association between depression and metabolic syndrome: a systematic review and meta-analysis of epidemiological studies. *Diabetes Care* 2012; 35: 1171–1180.
31. Lamia KA, Papp SJ, Yu RT, et al. Cryptochromes mediate rhythmic repression of the glucocorticoid receptor. *Nature* 2011; 480: 552–556.
32. An L, Zhang YZ, Liu XM, et al. Total flavonoids extracted from xiaobuxin-tang on the hyperactivity of hypothalamic-pituitary-adrenal axis in chronically stressed rats. *Evid Based Complement Alternat Med* 2011; 2011: 367619.
33. Zulkafli IS, Waddell BJ and Mark PJ. Postnatal dietary omega-3 fatty acid supplementation rescues glucocorticoid-programmed adiposity, hypertension, and hyperlipidemia in male rat offspring raised on a high-fat diet. *Endocrinology* 2013; 154: 3110–3117.
34. Mercau ME, Repetto EM, Perez MN, et al. Moderate exercise prevents functional remodeling of the anterior pituitary gland in diet-induced insulin resistance in rats: role of oxidative stress and autophagy. *Endocrinology* 2016; 157: 1135–1145.
35. da Fonseca TS, da Silva GF, Tanomaru-Filho M, et al. In vivo evaluation of the inflammatory response and IL-6 immunoexpression promoted by Biodentine and MTA Angelus. *Int Endod J* 2016; 49: 145–153.
36. Tuttolomondo A, La Placa S, Di Raimondo D, et al. Adiponectin, resistin and IL-6 plasma levels in subjects with diabetic foot and possible correlations with clinical variables and cardiovascular co-morbidity. *Cardiovasc Diabetol* 2010; 9: 50.
37. Hsu DC, Ma YF, Hur S, et al. Plasma IL-6 levels are independently associated with atherosclerosis and mortality in HIV-infected individuals on suppressive antiretroviral therapy. *AIDS* 2016; 30: 2065–2074.
38. Saremi A, Anderson RJ, Luo P, et al. Association between IL-6 and the extent of coronary atherosclerosis in the veterans affairs diabetes trial (VADT). *Atherosclerosis* 2009; 203: 610–614.

39. Zhang Q, Zhao K, Shen Q, et al. Tet2 is required to resolve inflammation by recruiting Hdac2 to specifically repress IL-6. *Nature* 2015; 525: 389–393.
40. Park EJ, Lee JH, Yu GY, et al. Dietary and genetic obesity promote liver inflammation and tumorigenesis by enhancing IL-6 and TNF expression. *Cell* 2010; 140: 197–208.
41. Wu J, Peng D, Li Z, et al. Network intrusion detection based on a general regression neural network optimized by an improved artificial immune algorithm. *PLoS One* 2015; 10: e0120976.
42. Maurer JM, Steele VR, Edwards BG, et al. Dysfunctional error-related processing in female psychopathy. *Soc Cogn Affect Neurosci* 2016; 11: 1059–1068.
43. Zeller T, Krankenberg H, Erglis A, et al. A randomized, multi-center, prospective study comparing best medical treatment versus best medical treatment plus renal artery stenting in patients with hemodynamically relevant atherosclerotic renal artery stenosis (RADAR) – one-year results of a pre-maturely terminated study. *Trials* 2017; 18: 380.
44. Chen IC, Lee CH, Chao TH, et al. Impact of routine coronary catheterization in low extremity artery disease undergoing percutaneous transluminal angioplasty: study protocol for a multi-center randomized controlled trial. *Trials* 2016; 17: 112.